Phason motion of a two-dimensional domain wall network: effective mass, interactions and effect of anharmonicity

1990 J. Phys.: Condens. Matter 2 4099

(http://iopscience.iop.org/0953-8984/2/18/006)

J. Phys.: Condens. Matter 2 (1990) 4099–4110. Printed in the UK

Phason motion of a two-dimensional domain wall network: effective mass, interactions and effect of anharmonicity

Neil D Shrimpton†‡ and Béla Joós§

Ottawa–Carleton Institute for Physics, University of Ottawa Campus, Ottawa, Ontario, Canada K1N 6N5

Abstract. We examine the phason dynamics of a two-dimensional honeycomb network of domain walls which is most clearly seen in the lowest vibrational mode of the network, the breathing mode.The motivating system is the incommensurate phase of krypton on graphite. Under the harmonic approximation for the krypton–krypton interaction, the effective mass, and strain field interactions between domain walls are identified. With this information, a renormalised model of the domain walls accurately matches the phason dynamics obtained from an adatom normal mode calculation. We then consider the anharmonic nature of the krypton–krypton interaction. The mass and interaction between domain walls are modified. We show that a normal mode calculation based on a quasi-harmonic approximation provides an inaccurate description of the phason dynamics.

1. Introduction

Solitons occur in many different physical systems and have stimulated numerous studies. Particularly well studied cases are those involving the sine–Gordon equation. The motivation for our study was to understand the dynamics of incommensurate monolayers. The applicability of the sine–Gordon equation to such systems was demonstrated first by Frank and van der Merwe (1949). Excellent reviews of the subject have been provided by Bak (1982) and Pokrovsky and Talapov (1984). An excellent review of the latest experimental work on the properties of the krypton on graphite system is provided by Specht *et al* (1987).

Our particular focus has been on the incommensurate solid phase of krypton on graphite. The structure of this system is shown in figure 1. This system is two-dimensional, with distinct soliton-like domain walls. Graphite has preferred adsorption sites that form a triangular lattice of spacing 1.42 Å, too close for krypton to achieve full occupancy. A more compatible spacing is 4.26 Å, the spacing of a $\sqrt{3} \times \sqrt{3}$ sublattice of adsorption sites. This fills every third substrate adsorption site and such a solid, commensurate with the substrate, has three possible centres with respect to the substrate. The incommensurate phase has a hexagonally symmetric superlattice of commensurate regions. Each region has neighbours centred about one of the three

† Present address: Department of Chemistry, The Pennsylvania State University, 152 Davey Laboratory, University Park, PA 16802, USA.

‡ Email address: NXS1@PSUVM (on BITNET).

§ Email address: BJOSJ@UOTTAWA (on BITNET).

0953-8984/90/184099+12$03.50

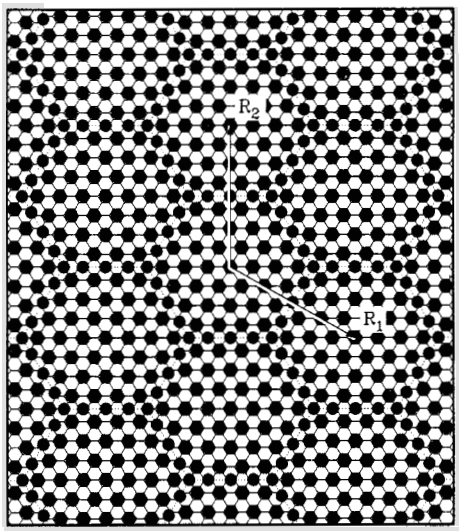

Figure 1. Stylised figure showing the positions of the adatoms in a krypton-on-graphite incommensurate monolayer. The full lines represent the bonds between carbon atoms in the substrate. The broken lines show the boundaries of the superlattice cell, while the vectors R_1 and R_2 are the primitive vectors of the superlattice (from Shrimpton and Joós 1990).

other adsorpton sites; the arrangement of such domains being such that a super-heavy domain wall separates each region (Kardar and Berker 1982).

Molecular dynamics studies (Abraham *et al* 1982, Abraham *et al* 1984), and normal mode calculations (Shrimpton *et al* 1986) reveal that the domain walls are highly mobile. A very low energy excitation due to a breathing of the domain wall lattice was found. This breathing mode preserves the total length of the domain walls (Villain 1980), and except for a repulsion between the strain fields of the vertices, would be degenerate in energy. The repulsion between the vertices causes the network to oscillate (breathe) about the equilibrium configuration. String-like vibrational modes of the domain walls are also apparent, and a renormalised model based on strings connected at vertices to form a honeycomb network has been developed (Shrimpton and Joós 1989). This renormalised model successfully describes the vibrational modes found through the adatom normal mode calculation (Shrimpton *et al* 1986).

This paper focuses on the low energy breathing mode. This mode represents the extension of the one-dimensional soliton motion to a two-dimensional network. In the following section we review the phason properties of the sine–Gordon equation and show how renormalised properties can be extracted. With this understanding, section 3 considers the honeycomb network of domain walls. Because our motivation is to model a real system for which the interatomic potentials are anharmonic (Shrimpton *et al* 1984), section 4 shows how anharmonicity affects the results of normal mode calculations.

2. 1D continuum theory

While the sine–Gordon equation has exact solutions (Forest and McLaughlin 1982),

the sine–Gordon equation itself provides only an approximate description of realistic systems. We therefore, in this section, focus only on the low energy phason dynamics of the system. The soliton solutions appropriate to incommensurate systems are kink chains. The solitons have mass and repel each other and low energy oscillations of the solitons have been shown to exist (McMillan 1977, Pokrovsky and Talapov 1978, Novaco 1980). We show in this section, how the mass and interaction between solitons can be extracted, and that this renormalised description is valid even when the solitons are strongly overlapped.

The potential energy U of the adatoms in the monolayer is given by

$$U = \frac{1}{2}\sum_{\boldsymbol{r},\boldsymbol{r}'} \Phi(\boldsymbol{r}-\boldsymbol{r}') + \sum_{\boldsymbol{g}} V_g[1-\cos(\boldsymbol{g}\cdot\boldsymbol{r})] \tag{1}$$

where $\boldsymbol{r}$ is the position of an adatom, Φ is the interaction potential between adatoms, and V_g is the corrugation of the substrate interaction. The first summation excludes the possibility of $\boldsymbol{r} = \boldsymbol{r}'$, and the second summation ranges over the first shell of adsorption site reciprocal lattice vectors.

It is useful to describe $\boldsymbol{r}$ as having a displacement $\boldsymbol{u}$ from the position $\boldsymbol{R}_c$ that the adatom would have if the monolayer was commensurate. For a uniaxial system of domain walls, $\boldsymbol{u}$ is perpendicular to and has variation perpendicular to a reciprocal lattice vector $\boldsymbol{g}$ of the adsorption sites. For simplicity and without loss of generality, the direction of $\boldsymbol{u}$ is taken to be in the x direction. By expanding Φ about $\boldsymbol{R}_c - \boldsymbol{R}_c'$ and by describing $u(x)$ in a continuum expansion, U is given to quadratic order in strain by

$$\frac{U}{N} = U_0 + \frac{\alpha}{4L}\int_0^L \frac{\partial u}{\partial x}\,\mathrm{d}x + \frac{\alpha+3\beta}{32L}\int_0^L \left(\frac{\partial u}{\partial x}\right)^2 \mathrm{d}x + 4V_g\left[1 - \frac{1}{L}\int_0^L \cos\left(\frac{2\pi u}{b_c}\right)\mathrm{d}x\right] \tag{2}$$

where

$$U_0 = \frac{1}{2}\sum_{\boldsymbol{R}_c}\Phi(|\boldsymbol{R}_c|) \qquad \alpha = \sum_{\boldsymbol{R}_c}\Phi'(|\boldsymbol{R}_c|)|\boldsymbol{R}_c| \qquad \beta = \sum_{\boldsymbol{R}_c}\Phi''(|\boldsymbol{R}_c|)|\boldsymbol{R}_c|^2.$$

N is the total number of adatoms, L is the distance between domain walls, and b_c is the spacing of the substrate adsorption sites. To minimise the energy, $u(x)$ must satisfy the integrated sine–Gordon equation

$$\frac{\alpha+3\beta}{32}\left(\frac{\partial u}{\partial x}\right)^2 = \tau - 4V_g\cos\left(\frac{2\pi u}{b_c}\right). \tag{3}$$

Because one domain wall causes a shift of one adsorption site

$$\int_0^L \frac{\partial u}{\partial x}\,\mathrm{d}x = -b_c \tag{4}$$

if the domain wall increases the density of the monolayer. On the other hand, if the domain wall decreases the density of the monolayer, the integral in (4) equals $+b_c$.

It is useful to define $\Lambda = (\alpha + 3\beta)/16$ and $\tau_c = 4V_g$. Given these values, the form and number of domain walls depends on the value of τ in equation (3). In particular the separation between domain walls L depends on τ as

$$L(\tau) = \int_0^{b_c} \left\{ \frac{2}{\Lambda} \left[\tau + \tau_c \cos\left(\frac{2\pi u}{b_c} \right) \right] \right\}^{-1/2} \mathrm{d}u. \tag{5}$$

It must be noted that L is not the distance between domain walls. Rather L is the distance across an equivalent number of atoms in the commensurate configuration. The actual distance between domain walls $L_x = L \pm b_c$, depending on whether or not the density of the monolayer is decreased or increased by the domain wall. For the sake of simplicity only the case $L_x = L - b_c$, where the density of the monolayer is increased, will be considered. As a further note, in the commensurate limit $L \to \infty$, the value of $\tau \to \tau_c$ in (5).

The Hamiltonian for the system of adatoms is given in the continuum approximation by

$$\frac{H}{N} = \frac{m}{2} \frac{1}{L} \int_0^L \dot{u}(x)^2 \, \mathrm{d}x + U/N. \tag{6}$$

Pokrovsky and Talapov (1984), (section 2.6) have solved this equation for the motion of the adatoms in the limit of infinitesimal oscillations. From this solution, the one dimensional system of domain walls has an acoustic mode with sound velocity

$$c = \sqrt{\frac{\Lambda}{m}} \sqrt{1 - k^2} \, \frac{K(k)}{E(k)} (1 - \epsilon) \tag{7}$$

where m is the mass per adatom, $k = 2\tau_c/(\tau + \tau_c)^{1/2}$, and $K(k)$ and $E(k)$ are complete elliptic integrals of the first and second kind. The additional factor of $1 - \epsilon$, with misfit $\epsilon = b_c/L$, accounts for the fact that the wavevector q is relative to the actual distance L_x over which the domain wall configuration is periodic.

In a renormalised description, the domain walls can be assigned a mass ρ per length, and an interaction energy $V(L_x)$ per length. For a given wavevector q, the domain walls vibrate with frequency

$$\omega = 2 \sqrt{\frac{V''(L_x)}{\rho}} \sin\left(\frac{qL_x}{2} \right) \tag{8}$$

from which, the sound velocity $c = (V''(L_x)/\rho)^{1/2} L_x$. To test the renormalised description, therefore, the effective mass ρ and the interaction potential $V(L_x)$ need to be determined and a comparison made with (7).

From equation (2), the energy per adatom U/N will be a function of τ. The effect of the vapour above the monolayer can be taken into account by subtracting from U/N the chemical potential μ of the vapour. The effective energy density of the monolayer is then $E_d = (U/N - \mu)/s$ where s is the area per adatom. Using (2)

$$E_d = \frac{1}{s} \left[U_0 - \mu + \tau_c - \tau + \frac{b_c}{L} \left(F(\tau) - \frac{\alpha}{4} \right) \right] \tag{9}$$

where

$$F(\tau) = \frac{\Lambda}{b_c}\int_0^{b_c}\left\{\frac{2}{\Lambda}\left[\tau + \tau_c\cos\left(\frac{2\pi u}{b_c}\right)\right]\right\}^{1/2} du. \tag{10}$$

The energy per domain wall length W which includes the domain wall interaction energy $V(L_x)$ is obtained from the difference in energy density between the incommensurate and commensurate monolayer configuration. The commensurate energy density is given by $E_c = (U_0 - \mu)/s_0$ where $s_0 = (3\sqrt{3}/2)b_c^2$ is the area per adatom of the commensurate configuration. The area per adatom of the incommensurate configuration varies with the misfit ϵ as $s = (1-\epsilon)s_0$. The energy density difference is then

$$E_d - E_c = (b_c/sL)[F(\tau) - \tfrac{1}{4}\alpha + U_0 - \mu + (L/b_c)(\tau_c - \tau)] \tag{11}$$

and the energy per domain wall is $L_x L_y(E_d - E_c)$ where $L_x = L(1-\epsilon)$ is the distance between domain walls and L_y is the length of the domain walls. Given the fact that $sL = s_0 L_x$, the energy per domain wall length W is

$$W(\tau) = (b_c/s_0)[F(\tau) - \tfrac{1}{4}\alpha + U_0 - \mu + (L/b_c)(\tau_c - \tau)]. \tag{12}$$

The interaction potential $V(L_x)$ will be, within an additive constant, given by $W(\tau)$. Correspondingly, $V'(L_x) = (\partial W/\partial\tau)(\partial\tau/\partial L_x)$, and because (10) and (5) give $\partial F/\partial\tau = L(\tau)/b_c$

$$V'(L_x) = (\tau_c - \tau)/s_0. \tag{13}$$

To obtain $V''(L_x)$ it is necessary to know $\partial\tau/\partial L_x$. From (5) and given the properties of elliptic integrals of the third type,

$$\frac{\partial L_x}{\partial\tau} = \frac{\partial L}{\partial\tau} = -\frac{b_c F(\tau)}{4(\tau+\tau_c)(\tau-\tau_c)} \tag{14}$$

so

$$V''(L_x) = \frac{4}{b_c s_0}\frac{(\tau+\tau_c)(\tau-\tau_c)}{F(\tau)} \tag{15}$$

The mass ρ per domain wall length can be determined from the kinetic contribution to the Hamiltonian in equation (6). Because the domain walls can be translated by shifting the origin in the renormalised description, $\partial u(x+X(t))/\partial t = \dot{X}\,\partial u/\partial x$ †, and the domain wall has an effective kinetic mass per length of

$$\rho = \frac{m}{s_0}\int_0^L\left(\frac{\partial u}{\partial x}\right)^2 dx \tag{16}$$

which by (10) can be expressed as $\rho = mb_c F(\tau)/(\Lambda s_0)$. Given the form for $V''(L_x)$ in (15) the sound velocity is

$$c = \frac{2}{b_c}\sqrt{\frac{\Lambda}{m}}\frac{\sqrt{(\tau+\tau_c)(\tau-\tau_c)}L_x(\tau)}{F(\tau)} \tag{17}$$

† u is also a function of $\dot{X}(t)$. This equation is only accurate in the limit of low velocity.

Because $F(\tau) = 2/\pi[2\Lambda(\tau+\tau_c)]^{1/2}E(k)$ and $L_x(\tau) = b_c/\pi[2\Lambda/(\tau+\tau_c)]^{1/2}K(k)(1-\epsilon)$ with $k = [2\tau_c/(\tau+\tau_c)]^{1/2}$ the renormalised description agrees with the exact solution (7) regardless of whether the domain walls are distinctly separated or not. Moreover, this process can be repeated with the substrate potential of (2) replaced by a more general periodic function of $2\pi u/b_c$; the resulting renormalised description matches the general result also given in section 2.6 of Pokrovsky and Talapov (1984).

With this understanding, the two-dimensional case can be considered. In the acoustic limit, the renormalised model must match the dispersion curves of the adatom normal mode calculation. If the renormalised model continues to match the dispersion curves for wavevectors away from the acoustic limit then the domain walls are sufficiently distinct that a renormalised model is valid. As will be evident, there can be significant overlap of the domain walls and an accurate renormalised description of the domain wall motion can still be obtained.

3. Honeycomb domain wall network

While a system of parallel commensurate domains is a possible configuration for an incommensurate monolayer, this is not the only possibility. The configuration of the monolayer can also be a hexagonal superlattice of commensurate domains. The domain walls then form a honeycomb network. This configuration is in general energetically favoured. The dynamics of this system have been studied, and a renormalised model has been constucted which accurately matches the motion of the domain wall lattice (Shrimpton and Joós 1989).

The renormalised model shows that the dynamics of the domain wall lattice can be described in terms of string oscillators which are attached at vertices to form a honeycomb network. The vertices are flexible rotators which interact with each other. Most vibrational modes depend on the string characteristics, the vertex dynamic behaviour, and the vertex interactions. The lowest energy mode, on the other hand, involves simply the kinetic mass of the domain wall network and the pair wise interaction between vertices. This mode is commonly known as the breathing mode, and is comparable to the vibrational mode of the one-dimensional case discussed in the preceding section.

Both the kinetic mass and the vertex pair interaction can be determined from the domain wall profile and energy of the static incommensurate monolayer. The vibrational behaviour of the breathing mode can be determined from this renormalised information and a comparison made with the adatom normal mode calculations. The renormalised model predicts that the dispersion curve associated with the breathing mode should vary as

$$\omega(\boldsymbol{q}) = 2\sqrt{(3b/2M)(1-a_1^R(\boldsymbol{q}))} \tag{18}$$

where

$$a_1^R(\boldsymbol{q}) = \frac{2}{27(1-\xi^2)}[3-\cos(\boldsymbol{q}\cdot\boldsymbol{R}_{12})-\cos(\boldsymbol{q}\cdot\boldsymbol{R}_{23})-\cos(\boldsymbol{q}\cdot\boldsymbol{R}_{31})] \tag{19}$$

and

$$\xi = \tfrac{1}{3}\sqrt{3+2\cos(\boldsymbol{q}\cdot\boldsymbol{R}_1)+2\cos(\boldsymbol{q}\cdot\boldsymbol{R}_2)+2\cos(\boldsymbol{q}\cdot\boldsymbol{R}_3)}.$$

$\boldsymbol{R}_i$ are first-shell reciprocal lattice vectors of the superlattice, $\boldsymbol{R}_{ij} = \boldsymbol{R}_i - \boldsymbol{R}_j$, $b = V''(L)$ is the second derivative of the vertex to vertex strain field interaction, and M is the effective mass per domain associated with the domain walls. The form (18) accurately matches that found from adatom normal mode calculations for the dispersion curve of the breathing mode, and the value $3b/2M$ can be fitted as a parameter.

The kinetic mass of the domain wall network can be obtained from the static profile of the adatoms. As done in previous work (Shrimpton *et al* 1984), the positions of the adatoms $\boldsymbol{r}$ can be described as having a shift $\boldsymbol{u}$ from a triangular lattice of averaged positions $\boldsymbol{R}$. With the assumption of superlattice periodicity,

$$\boldsymbol{u}(\boldsymbol{R}) = \sum_{l,m} \boldsymbol{u}_{lm} \exp(\mathrm{i}\boldsymbol{q}_{lm} \cdot \boldsymbol{R}) \tag{20}$$

where the vectors $\boldsymbol{R}$ form a triangular lattice with spacing and angle determined by the density and orientation of the monolayer, and the summation proceeds over all reciprocal lattice vectors $\boldsymbol{q}_{lm}$ of the superlattice. The vectors $\boldsymbol{R}$ can be related to the $\sqrt{3} \times \sqrt{3}$ lattice of commensurate vectors $\boldsymbol{R}_c$ by $\boldsymbol{R} = \mathbf{C}\boldsymbol{R}_c$. If the monolayer is not rotated $\mathbf{C}$ can be replaced by a scalar constant C. This will be assumed in the following.

If the positions of the adatoms $\boldsymbol{r}$ are described by shifts $\boldsymbol{u}_c(\boldsymbol{R}_c)$ from commensurate positions $\boldsymbol{R}_c$ then

$$\boldsymbol{u}_c(\boldsymbol{R}_c) = \boldsymbol{u}(C\boldsymbol{R}_c) + (C-1)\boldsymbol{R}_c. \tag{21}$$

The domain walls can then be moved across the monolayer by introducing a time dependent shift vector $\boldsymbol{X}(t)$ so that the adatoms have positions

$$\boldsymbol{r} = \boldsymbol{R}_c + \boldsymbol{u}_c(\boldsymbol{R}_c + \boldsymbol{X}(t)). \tag{22}$$

The kinetic energy E_K per superlattice domain, associated with the time variation of $\boldsymbol{X}(t)$, by (20), (21), and (22) has the form $\frac{1}{2}M\dot{X}^2$ where

$$M = Nm\left((C-1)^2 - \frac{1}{2}\sum_{l,m}(\boldsymbol{u}_{lm} \cdot \boldsymbol{u}_{lm})(\boldsymbol{q}_{lm} \cdot \boldsymbol{q}_{lm})\right) \tag{23}$$

is the kinetic mass per domain, N is the number of adatoms per domain and m is the mass per adatom.

The vertex to vertex interaction can be determined from static results of how the energy density E of the monolayer varies with coverage. The energy per domain associated with the domain walls is $(3\sqrt{3})/2L^2(E(\epsilon) - E(0))$, where $E(\epsilon)$ is the energy density and $L = b_c(1/\epsilon - 1)/\sqrt{3}$ is the length per side of the domain. The energy associated with the domain walls can be broken into terms constant in L which provide the energy per vertex, terms linear in L which provide the energy per length of domain walls, and non-linear terms which provide the strain field interactions within the monolayer. The dominant strain field interaction is that between vertices. The domain wall to domain wall interaction is carried across the commensurate domains and is damped out exponentially. The vertex to vertex interaction, on the other hand, extends along the domain walls. Because the adatoms on the domain walls are not

near registry with the substrate, the substrate does not influence the vertex to vertex interaction. Its range is limited only by adatom pair interactions and, similar to strain field interactions in elastic media, its decay is algebraic. The source of the interaction is the focused displacement fields of the domain walls when they intersect at the vertex. This focusing creates a density extreme, which is eased by a vertex strain field. The intersection of the vertex strain fields results in a vertex to vertex interaction.

A hexagonally symmetric incommensurate monolayer was studied for a variety of coverages. The method of calculation for the energy of the monolayer has been presented previously (Shrimpton *et al* 1984), as has been the method of calculating monolayer dynamics (Shrimpton *et al* 1986). Because the dynamical information is obtained under a quasi-harmonic approximation, to make the comparison with the renormalised prediction accurate, the adatom interactions were described by a nearest neighbour pair interaction $\Phi(r)$ with form

$$\Phi(r) = \begin{cases} a_0 + a_1(r - r_c) + a_2(r - r_c)^2 & \text{if } r \leq r_c \\ 0 & \text{otherwise.} \end{cases} \tag{24}$$

The values $a_0 = -163.75$ K, $a_1 = 120.01$ K Å^{-1}, $a_2 = 112.42$ K Å^{-2}, and $r_c = 4.26$ Å were chosen because they match in the commensurate limit the krypton–krypton pair interaction.

The substrate interaction was modelled by the potential

$$V(\boldsymbol{r}) = V_0 + \sum_{\boldsymbol{g}} V_g[1 - \exp(\mathrm{i}\boldsymbol{g} \cdot \boldsymbol{r})] \tag{25}$$

where $\boldsymbol{r}$ is the lateral position of the adatom. For physisorbed monolayers, to a good approximation, the summation can be restricted to the first shell of the substrate adsorption site reciprocal lattice vectors $\boldsymbol{g}$ (Steele 1973). Equation (25) introduces the variable V_g, known as the substrate corrugation, which gives the non-uniformity of the substrate interaction. In order to make the domain walls broad enough that pinning effects are insignificant, the substrate corrugation was taken to be 2.0 K. Under such circumstances the monolayer is essentially an elastic media: The analysis represents a direct extension of the one-dimensional sine–Gordon equation, to a two-dimensional system with hexagonal periodicity.

The average energy per adatom, resulting from the calculation, as a function of the monolayers misfit is shown in figure 2. The three curves shown are least squares fits of either fifth- or sixth-order polynomials. Fit 1 is a sixth-order polynomial which takes into account all points up to a misfit of 4.5%. Fit 2 is a fifth-order polynomial which takes into account all points up to a misfit of 3.1%. Fit 3 is a fifth-order polynomial which takes into account all points up to 3.0%. As shown in figure 2, they all follow the data extremely well, and given the resolution they are indistinguishable. While higher order polynomial fits over more restricted ranges could be performed, this was not useful because the data have calculational inaccuracies which must be smoothed.

If the average energy per adatom U/N varies with the misfit ϵ as

$$U/N = \mu_c - \mu + c_1\epsilon + c_2\epsilon^2 + c_3\epsilon^3 + c_4\epsilon^4 + c_5\epsilon^5 + c_6\epsilon^6 \tag{26}$$

the change in the vertex interaction potential $V''(L)$ is given by

$$V''(L) = 2c_3\epsilon^3 + 6c_4\epsilon^4 + 12c_5\epsilon^5 + 20c_6\epsilon^6. \tag{27}$$

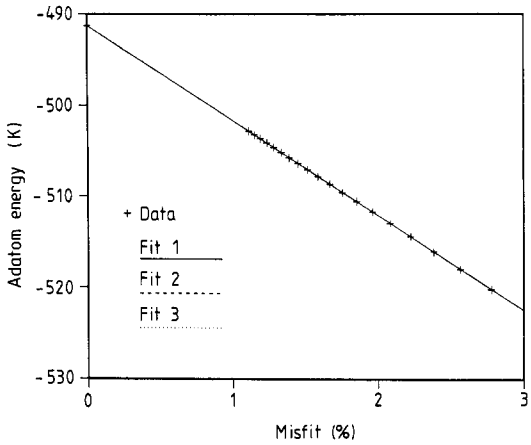

Figure 2. Energy per adatom as a function of misfit for a monolayer with adatoms that interact with potential (24) when the substrate corrugation is 2.0 K. There are 3 polynomial fits to the data. As shown they are indistinguishable.

The mass of the domain walls per domain is determined by (23) from the structure of the incommensurate monolayer. The normal mode calculation provides the dispersion relation for the breathing mode. The dispersion information is accurately matched by the form predicted from equation (18). The value of $3b/2M$ is extracted as a parameter fit. This value as well as the effective mass, and the values $3V''(L)/2M$ obtained from the three possible fits to (26) are shown in table 1. It is clear that within the variability of the polynomial fit, the renormalised description of the domain wall dynamics agrees with the adatom normal mode results. As expected from the previous section, the renormalised model is applicable even at misfits as great as 3.03%. At this density, the domain walls are so overlapped that the structure of the incommensurate phase is more that of a modulated solid than a network of domain walls.

Table 1. Vertex interaction parameters $3b/2M$ obtained from dynamic information, and the corresponding values of $3V''(L)/2M$ calculated for a variety of monolayer misfits when the adatom pair interaction is a nearest neighbour harmonic polynomial and the substrate corrugation is 2.0 K. ϵ gives the misfit of the monolayer, M is the calculated kinetic mass per domain.

ϵ (%)	M (10^{25} kg)	$\frac{3}{2}V''(L)/M$ (10^{21} s^{-2}) Fit 1	Fit 2	Fit 3	$\frac{3}{2}b/M$ (10^{20} s^{-2})
3.03	0.694	4.224	4.736	8.829	47.64
2.78	0.754	2.511	2.439	3.817	26.78
2.56	0.818	1.517	1.334	1.658	15.80
2.38	0.885	0.936	0.775	0.725	9.59
2.22	0.953	0.586	0.482	0.325	5.90
2.08	1.022	0.378	0.325	0.171	3.68
1.96	1.093	0.254	0.232	0.118	2.35

4. Anharmonic effects

Theories to describe the properties of domain wall networks rely heavily on the assumption that the adatom interaction is harmonic. However, this assumption is not generally valid when dealing with real systems (Shrimpton *et al* 1984, Gordon and Lançon 1985). Dynamic information for domain wall lattices can be obtained from molecular dynamics simulations. However, the large size of the domain wall system, and the long time scales for domain wall motion make such calculations difficult. Normal mode calculations can be performed to obtain phason information, except that anharmonicity is incorporated only in a quasi-harmonic sense. Because this method was used to obtain dynamic information for the domain wall lattice, this section presents a comparison with the renormalised model for the anharmonic system of krypton on graphite. The potentials used have been described in a previous paper (Shrimpton *et al* 1984) and the substrate corrugation is taken to be 7.0 K, a typical value. The form (18) fits the normal mode dispersion data accurately, and the value $3b/2M$ is extracted as a parameter.

As before, the vertex interaction potential $V(L)$ is determined from static results of how the energy of the monolayer varies with density. From previous work (Shrimpton *et al* 1988), the energy density E of the incommensurate monolayer is known to vary with misfit ϵ as

$$E(\epsilon) = \frac{2}{3\sqrt{3}b_c^2}\left(\frac{\mu_c - \mu}{(1-\epsilon)^2} + E_0 - \mu_c + 2A^{-1/\beta}\int_0^{\epsilon}\frac{x^{1/\beta}}{(1-x)^3}\,dx\right) \tag{28}$$

where b_c is the spacing of the substrate adsorption sites, μ_c is the chemical potential of the commensurate monolayer, μ is the chemical potential of the vapour above the monolayer, E_0 is the energy per adatom of the commensurate monolayer, and A and β are additional fitting parameters related to how the misfit of the monolayer varies with chemical potential. The value of $V''(L)$ extracted from this varies with misfit as

$$V''(L) = \frac{2A^{-1/\beta}}{3b_c^2}\left(2\int_0^{\epsilon}\frac{x^{1/\beta}}{(1-x)^3}\,dx + \frac{\epsilon^{1+1/\beta}[(1-\epsilon)/\beta - 2 + \epsilon]}{(1-\epsilon)^2}\right). \tag{29}$$

From (23) the mass associated with the domain walls is obtained. To assess the effect of anharmonicity on the domain wall mass, an effective domain wall density is calculated. Because the domain walls move perpendicular to their length, the kinetic mass M is not $3\rho L$. Instead the domain wall density ρ is related to the mass per domain M by $M = \frac{3}{2}\rho L$. For calculational purposes, the length of the domain wall segments L can be determined from the misfit ϵ of the monolayer by $L = (1/\epsilon - 1)$ 1.42 Å. The values of M and ρ are shown in table 2 for a variety of monolayer densities. As the misfit is decreased, the density ρ tends to that of an isolated domain wall. From section 2 a domain wall density can also be obtained. In the commensurate limit, $\rho = 8m/(3\pi d_c)(4V_g/\Lambda)^{1/2}$. For krypton, $m = 1.391 \times 10^{-25}$ kg is the mass per krypton adatom, and $d_c = 4.26$ Å is the commensurate lattice spacing. The commensurate value of $\Lambda = 4781.97$ K, and when the substrate corrugation is $V_g = 7.0$ K, $\rho = 2.12 \times 10^{-17}$ kg m^{-1}. It is clear that after extrapolating the values of ρ in table 2 the domain wall density ρ is less than 2.12×10^{-17} kg m^{-1}. Anharmonicity decreases the effective mass of the domain walls, a fact in agreement with Gordon and Lançon (1985) who found that the anharmonic nature of the adatom interaction

Table 2. Vertex interaction parameters $3b/2M$ for a variety of misfits obtained from dynamic information compared to $3V''(L)/2M$ obtained from the renormalized description for a monolayer of krypton on graphite, when the substrate corrugation is 7.0 K. M is the kinetic mass per domain, ρ is the mass per domain wall length.

ϵ (%)	M (10^{-25} kg)	ρ (10^{-17} kg m^{-1})	$\frac{3}{2}b/M$ (10^{20} s^{-2})	$\frac{3}{2}V''(L)/M$ (10^{21} s^{-2})
3.33	0.711	1.113	5.64	6.77
3.03	0.792	1.127	1.35	3.50
2.78	0.876	1.143	0.49	1.92
2.56	0.963	1.160	1.23	1.09
2.38	1.051	1.175	1.46	0.66
2.22	1.140	1.189	0.57	0.41
2.08	1.229	1.202	0.26	0.26
1.96	1.319	1.214	~ 0.14	0.17
1.85	1.408	1.224	~ 0.07	0.12

broadens the domain walls and effectively increases the elastic constants required to describe the domain wall profiles.

The values $A = 1.778$ and $\beta = 0.210$, to be used in (29) are obtained from fitting (28) to the calculated energy variation with density. These numbers do not compare with $A = 0.079$ and $\beta = 0.33$, found from experiment (Stephens *et al* 1984) because zero point motion of the adatoms should not be included in the calculation (Shrimpton *et al* 1988). From calculations of the potential energy of the incommensurate monolayer, the values of $A = 1.778\%$ and $\beta = 0.210$. This is different from the experimental results because the zero point motion of the adatoms is not considered. It is clear from table 2 that the value of $3V''(L)/2M$ obtained from the renormalised description does not agree with the parameter value $3b/2M$ obtained from the normal mode calculation. The value of $V''(L)$ calculated from the variation in energy density is much larger than the value of b required to fit the dynamic information. That these two values do not agree reflects the fact that they do not contain the same information. The krypton–krypton interaction is anharmonic, and the effective quasi-harmonic constants of the adatoms vary significantly with spacing. To draw from the 1D continuum results, if U_0, α and Λ vary with L in equation (11) then the sound velocity c of (7) will not match $(V''(L_x)/\rho)^{1/2}L_x$. Correspondingly, the dynamically derived parameter b for the domain wall network does not contain information about the changing elastic nature of the adatoms while $V''(L)$ does.

5. Conclusion

Similar to one-dimensional cases, two-dimensional networks of domain walls have phason dynamics. The domain walls have an effective mass, and the lowest energy vibration of the domain wall lattice is controlled by a vertex to vertex strain field interaction. This interaction can be renormalised as a vertex–vertex pair potential. This potential together with the effective domain wall mass can be used in a renormalised model to calculate domain wall motion. If the monolayer is not an elastic medium, the domain wall motion obtained from an atomic normal mode calculation will not be accurate. This must be taken into account if the sine–Gordon equation, or its two-dimensional extension, is used via a quasi-harmonic approximation to study phason dynamics of realistic systems.

Acknowledgments

This work has been supported by the Natural Sciences and Engineering Research Council of Canada.

References

Abraham F F, Koch S W and Rudge W E 1982 *Phys. Rev. Lett.* **49** 1830
Abraham F F, Rudge W E, Auerbach D J and Koch S W 1984 *Phys. Rev. Lett.* **52** 445
Bak P 1982 *Rep. Prog. Phys.* **45** 587
Forest M G and McLaughlin D W 1982 *J. Math. Phys.* **73** 1248
Frank F C and van der Merwe J H 1949 *Proc. R. Soc.* A **198** 205
Gordon M B and Lançon F 1985 *J. Phys. C:Solid State Phys.* **18** 3929
Kardar M and Berker A N 1982 *Phys. Rev. Lett.* **49** 793
McMillan W L 1977 *Phys. Rev.* B **16** 4655
Novaco A D 1980 *Phys. Rev.* B **22** 1645
Pokrovsky V L and Talapov A L 1978 *Zh. Eksp. Teor. Fiz.* **78** 1151
—— 1984 *Theory of Incommensurate Crystals* (New York: Harwood Academic)
Shrimpton N D, Bergersen B and Joós B 1984 *Phys. Rev.* B **29** 6999
—— 1986 *Phys. Rev.* B **34** 7334
Shrimpton N D, Joós B and Bergersen B 1988 *Phys. Rev.* B **38** 2124
Shrimpton N D and Joós B 1990 *Phys. Rev.* B **40** 10564
Specht E D, Mak A, Peters C, Sutton M, Birgeneau R J, d'Amico K L, Moncton D E, Nagler S E and Horn P M 1987 *Z. Phys.* B **69** 347
Steele W A 1973 *Surf. Sci.* **36** 317
Stephens P W, Heiney P A, Birgeneau R J, Horn P M, Moncton D E and Brown G S 1984 *Phys. Rev.* B **29** 3512
Villain J 1980 *Ordering in Strongly Fluctuating Condensed Matter Systems* ed T Riste (New York: Plenum) p 221